Supplementary Information

Reconfigurable Multifunctional Ambipolar Polymer Transistors with Improved Switching-off Capability Upon Non-Uniformly Distributed Compensation Potential

Peng Wei, Xudong Wang, Xianglong Li, Nan Qiao, Songyu Han, Peng Zhang, Yunfeng Deng, Wei Zhang, Laju Bu and Guanghao Lu*

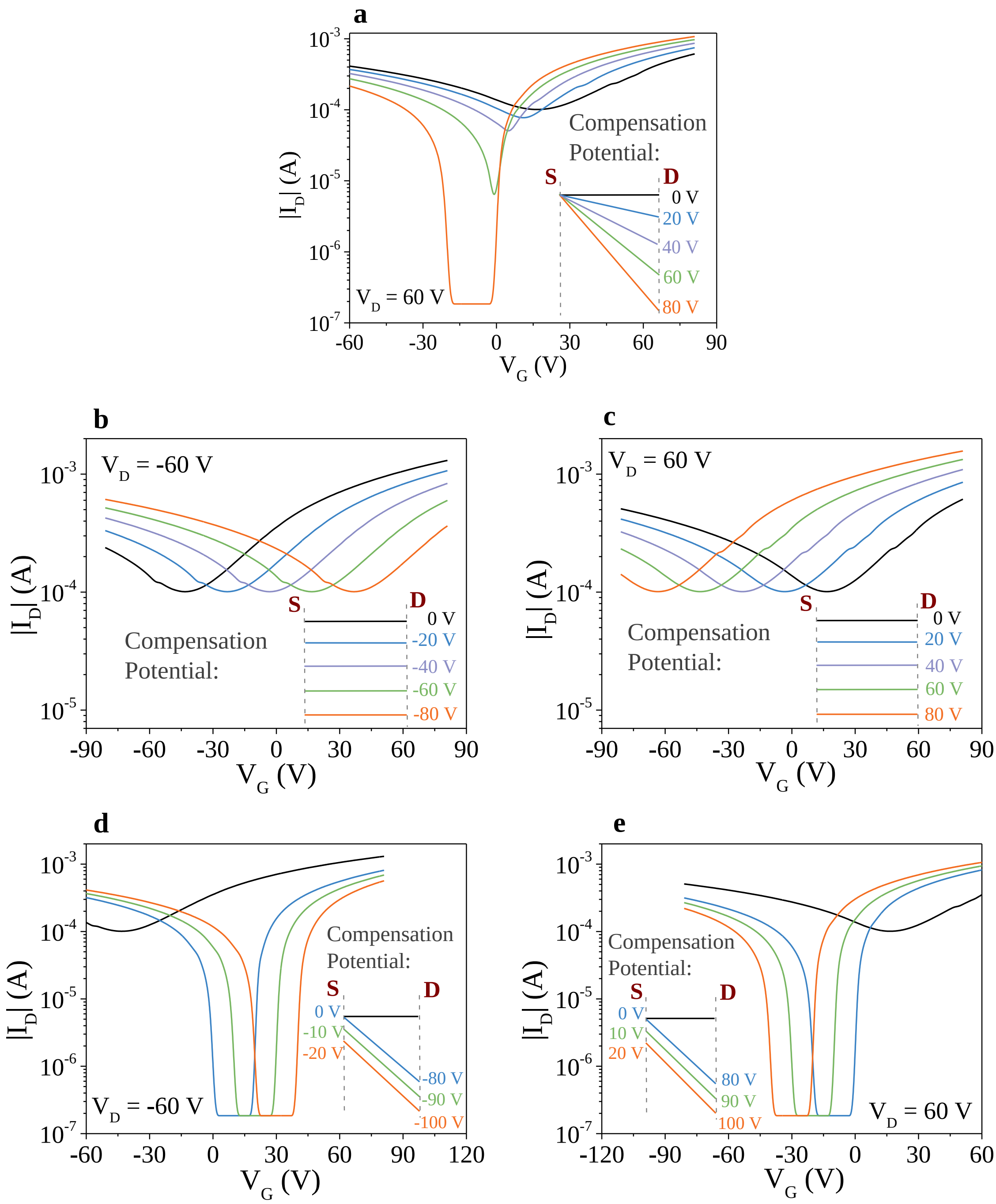

Supplementary Figure 1. Simulated transfer characteristics of the ambipolar transistor under compensation fields with different potential gradient along the channel. a Simulated transfer characteristics of the ambipolar transistor under linearly varied compensation potentials with different gradient along the channel. **b**, **c** Simulated transfer characteristics of the ambipolar transistor under uniform compensation potentials along the channel. **d**, **e** Simulated transfer characteristics of the ambipolar transistor under linearly varied compensation potentials with the same gradient and different value along the channel. The insets are the compensation potentials applied along the channel.

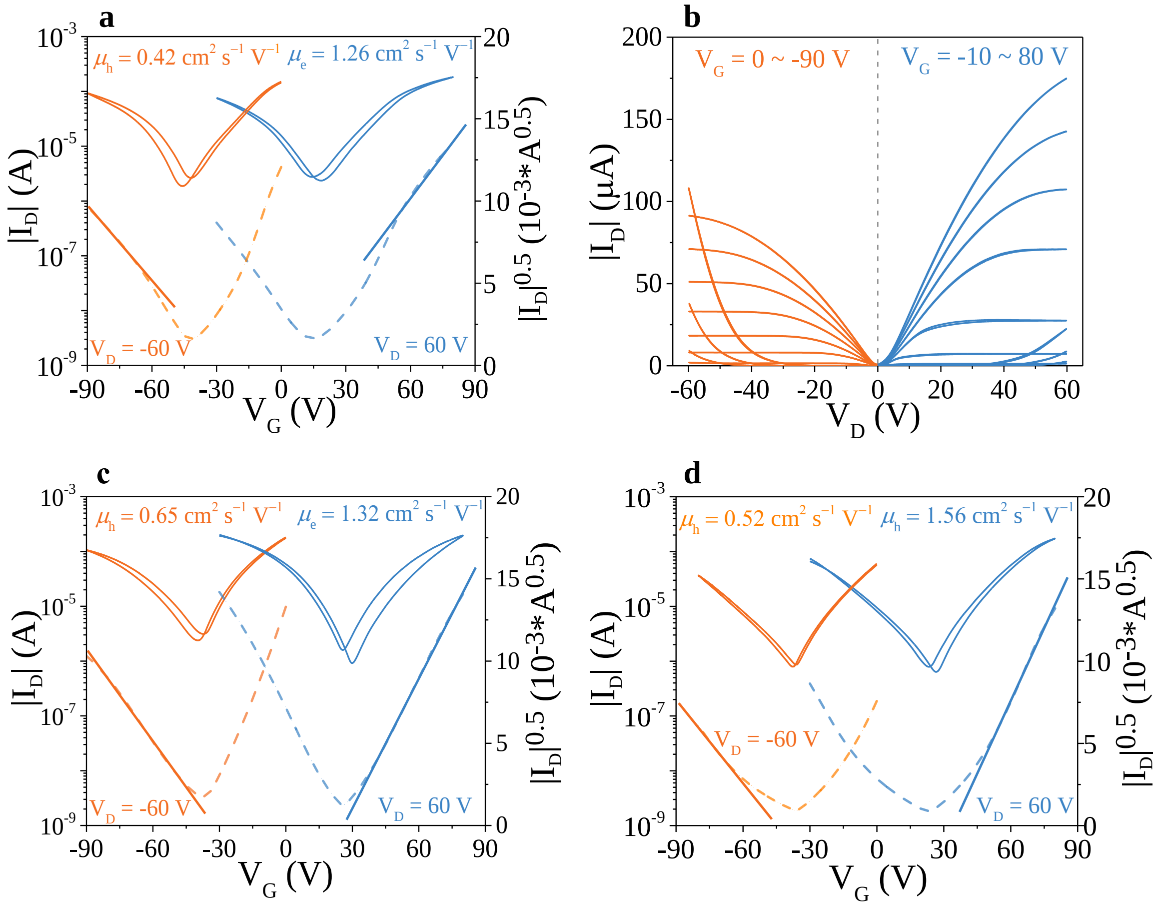

Supplementary Figure 2. Transistor performance of **a**, **b** pure PDPP-4FTVT, **c** PDPP-4FTVT$_{(5\%)}$@PS and **d** PDPP-4FTVT$_{(20\%)}$@PS films. 5% and 20% represent the weight ratios of PDPP-4FTVT in the blend films.

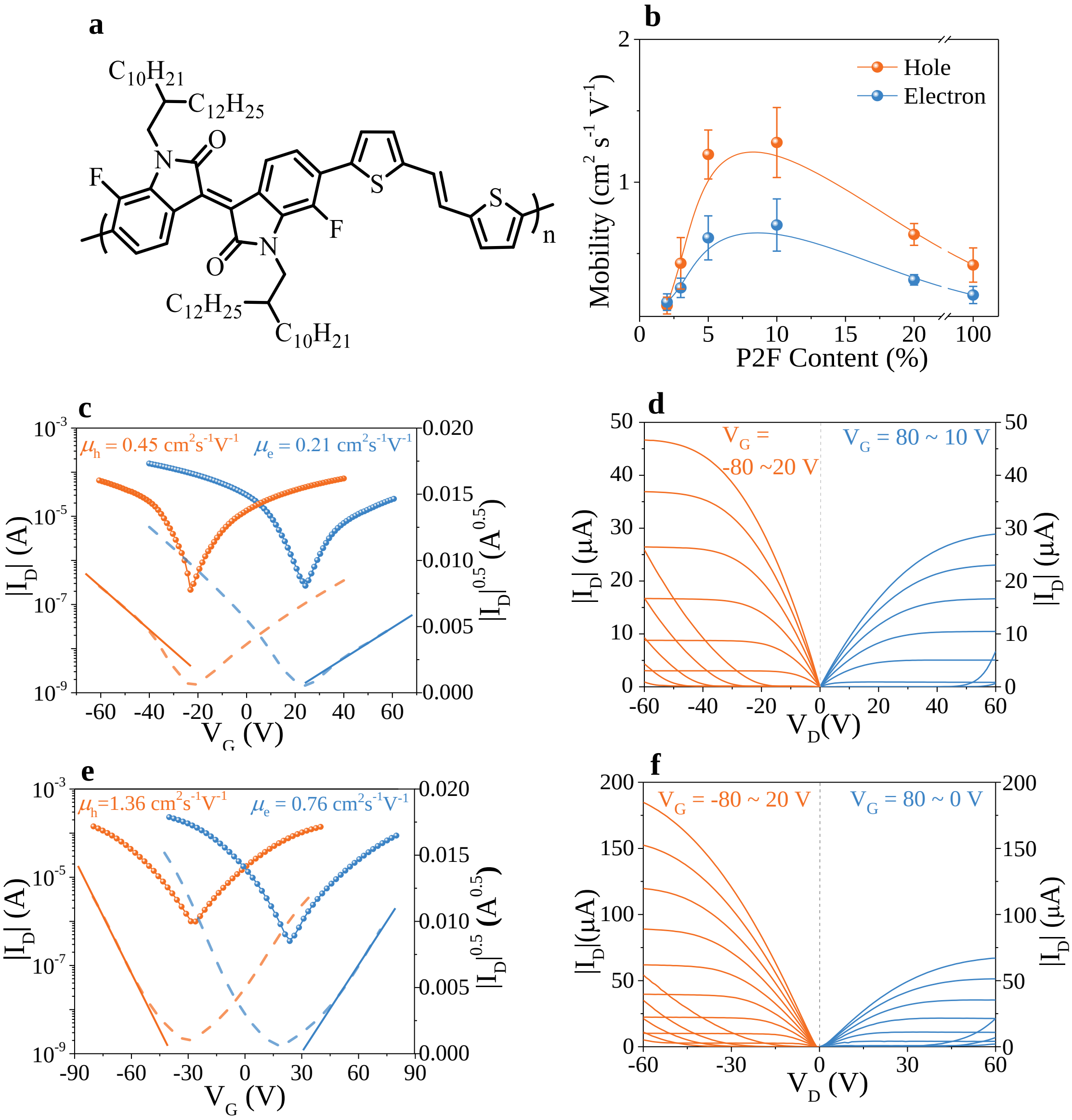

Supplementary Figure 3. Performance of P2F based ambipolar transistors. a Chemical structure of P2F. **b** Field-effect electron and hole mobility of the transistors based on P2F and P2F@PS blends. **c** Transfer and **d** output characteristics of pure P2F transistor. **e** Transfer and **f** output characteristics of $P2F_{10\%}$@PS transistor. The transfer curves in **c** and **e** were measured at V_d = -60 and 60 V for p-type and n-type respectively.

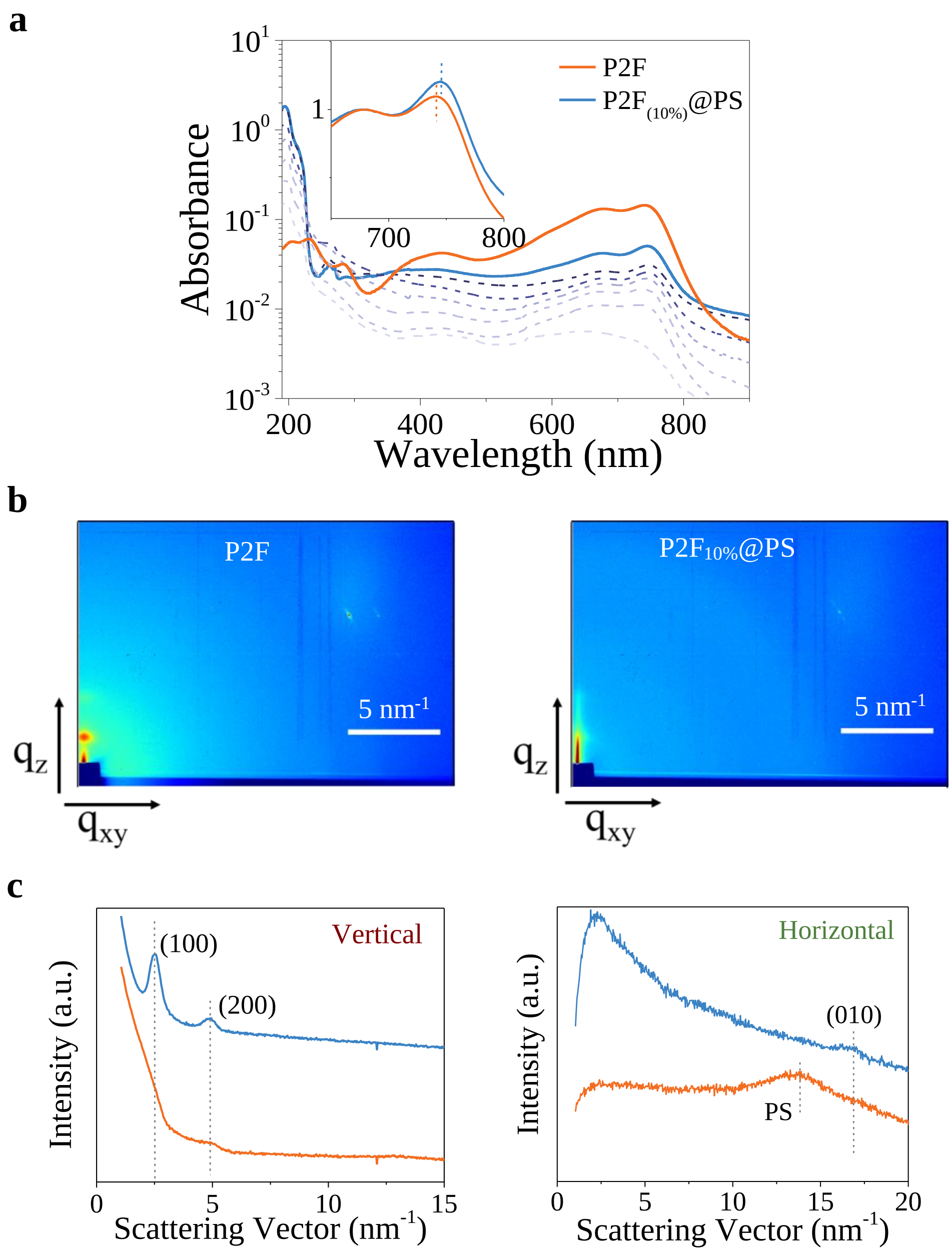

Supplementary Figure 4. Morphology/microstructure characterization of P2F and P2F$_{10\%}$@PS films. a Absorbance of P2F and P2F$_{10\%}$@PS blend. The dash lines are the absorbance of P2F$_{10\%}$@PS films after different time of oxygen plasma etching, which demonstrate there are no obvious vertical phase separations of conjugated polymers and insulators. **b** Typical GIWAXS 2D pattern and **c** 1D radially-integrated data of P2F and P2F$_{10\%}$@PS thin films. The blue and orange curves are attributed to the P2F and P2F$_{10\%}$@PS data, respectively.

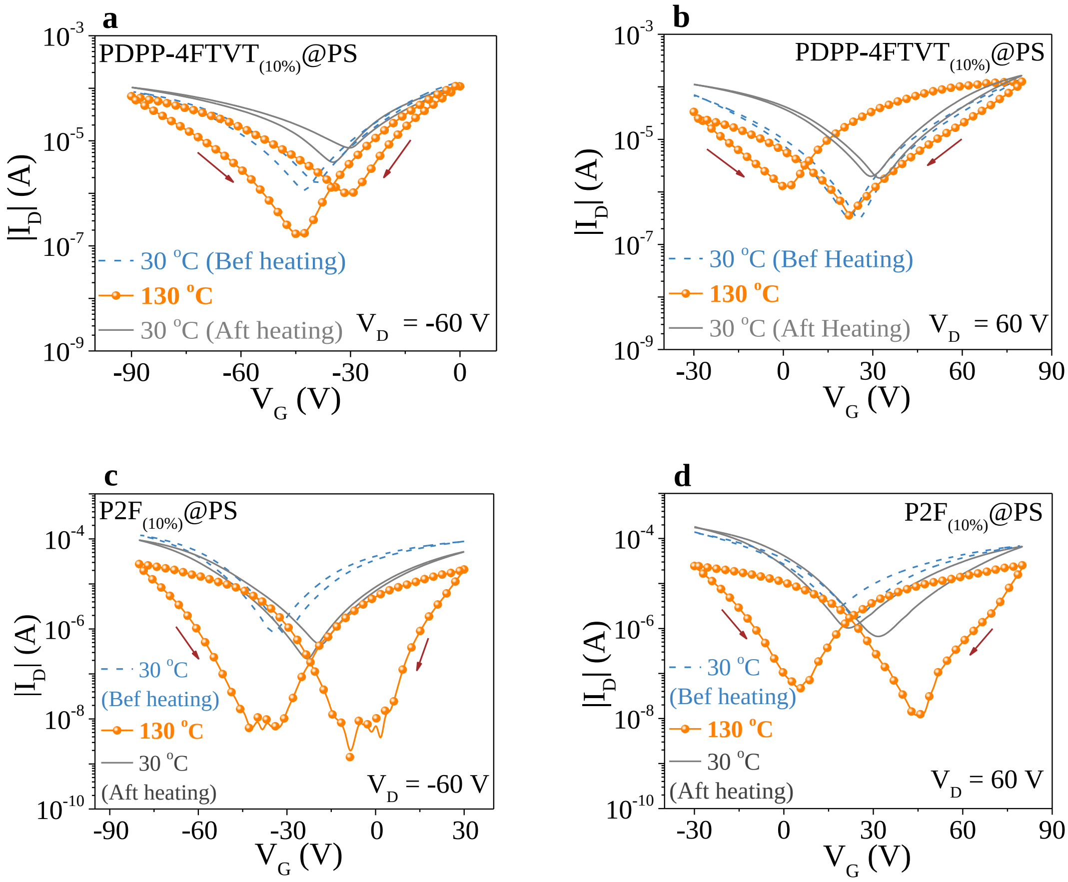

Supplementary Figure 5. Transfer characteristics of **a**, **b** PDPP-4FTVT$_{10\%}$@PS and **c**, **d** P2F$_{10\%}$@PS transistors measured before, at and after heating to 130 ºC.

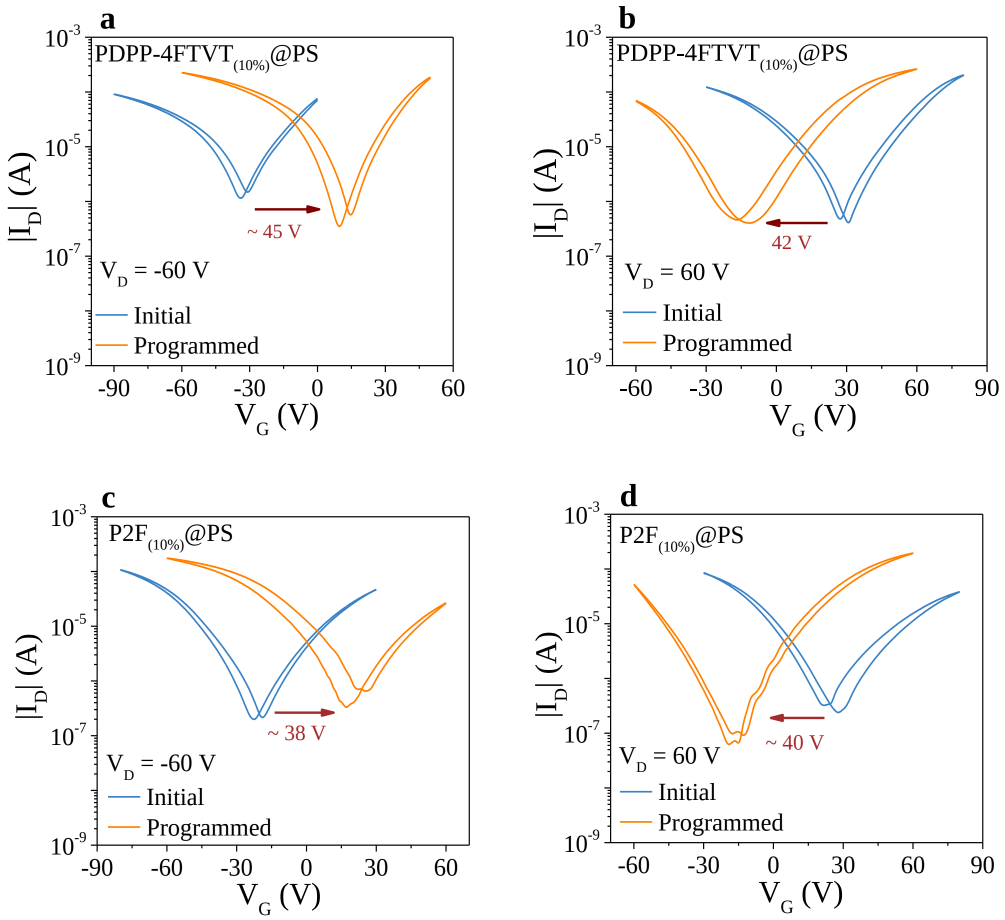

Supplementary Figure 6. Transfer characteristics of **a**, **b** PDPP-4FTVT$_{10\%}$@PS, and **c**, **d** P2F$_{10\%}$@PS transistors before and after introducing uniformly distributed electret charges along the channel by the gate stress of V_G = 90 V & V_D = 0 V (**a**, **c**), and V_G = -90 V & V_D = 0 V (**b**, **d**).

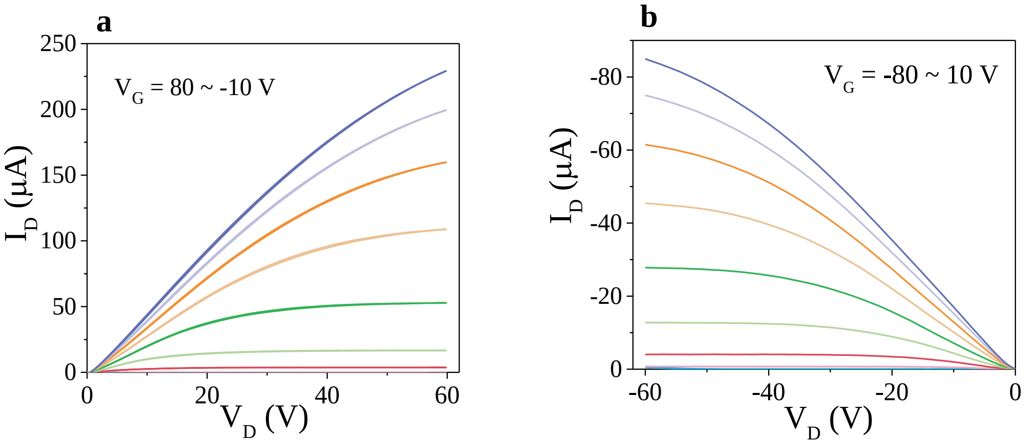

Supplementary Figure 7. Output characteristics of PDPP-4FTVT$_{10\%}$@PS transistor under **a** n-type operation, with electret charges injected by V_G = -20 V & V_D = 60 V, and **b** p-type operation, with electret charges injected by V_G = 20 V & V_D = -60 V.

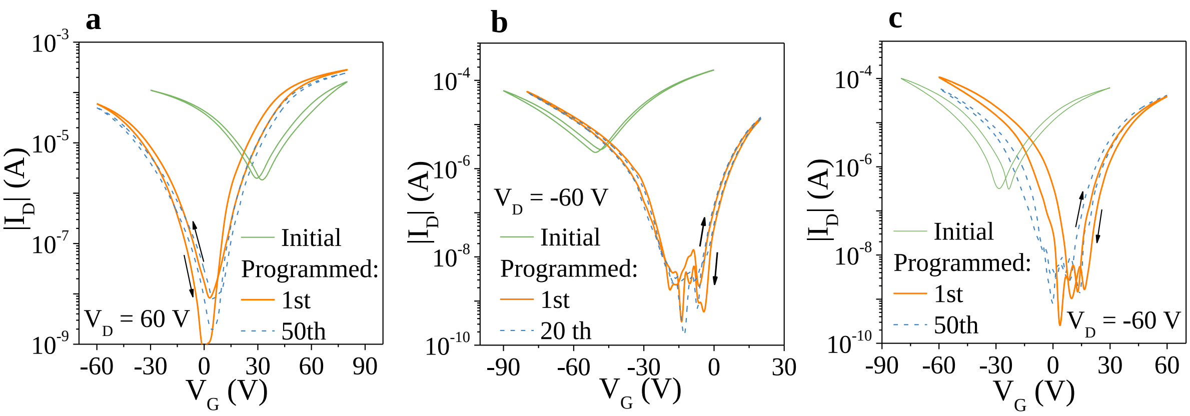

Supplementary Figure 8. Transfer characteristics of PDPP-4FTVT$_{10\%}$@PS transistor without and with non-uniformly distributed electret charges. The electret charges are injected by: **a** V_G = -20 V & V_D = 60 V, **b** V_G = 10 V & V_D = -80 V and **c** V_G = 40 V & V_D = -60 V.

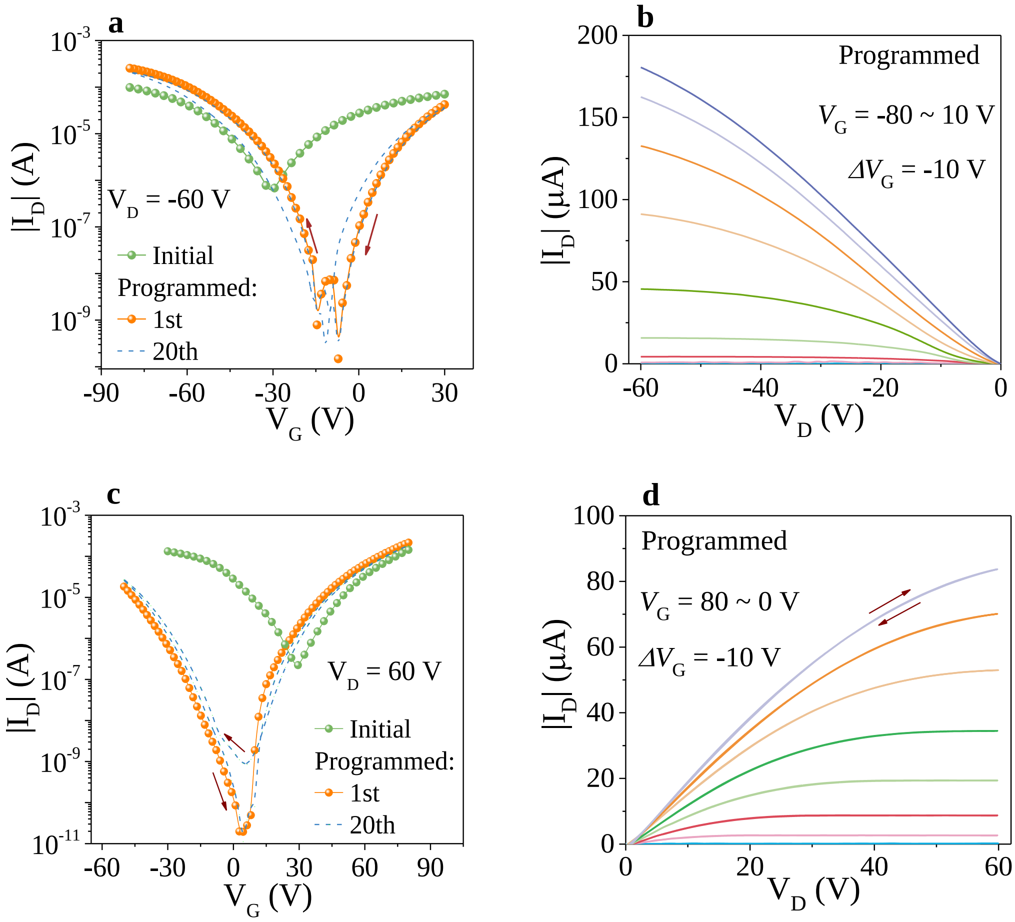

Supplementary Figure 9. Performance of ambipolar transistor based on P2F$_{10\%}$@PS with non-uniformly distributed electret charges. a Transfer and **b** output characteristics of P2F$_{10\%}$@PS transistor with electret charges injected by V_G = 20 V & V_D = -60 V. **c** Transfer and **d** output characteristics of P2F$_{10\%}$@PS transistor with electret charges injected by V_G = -20 V & V_D = 60 V.

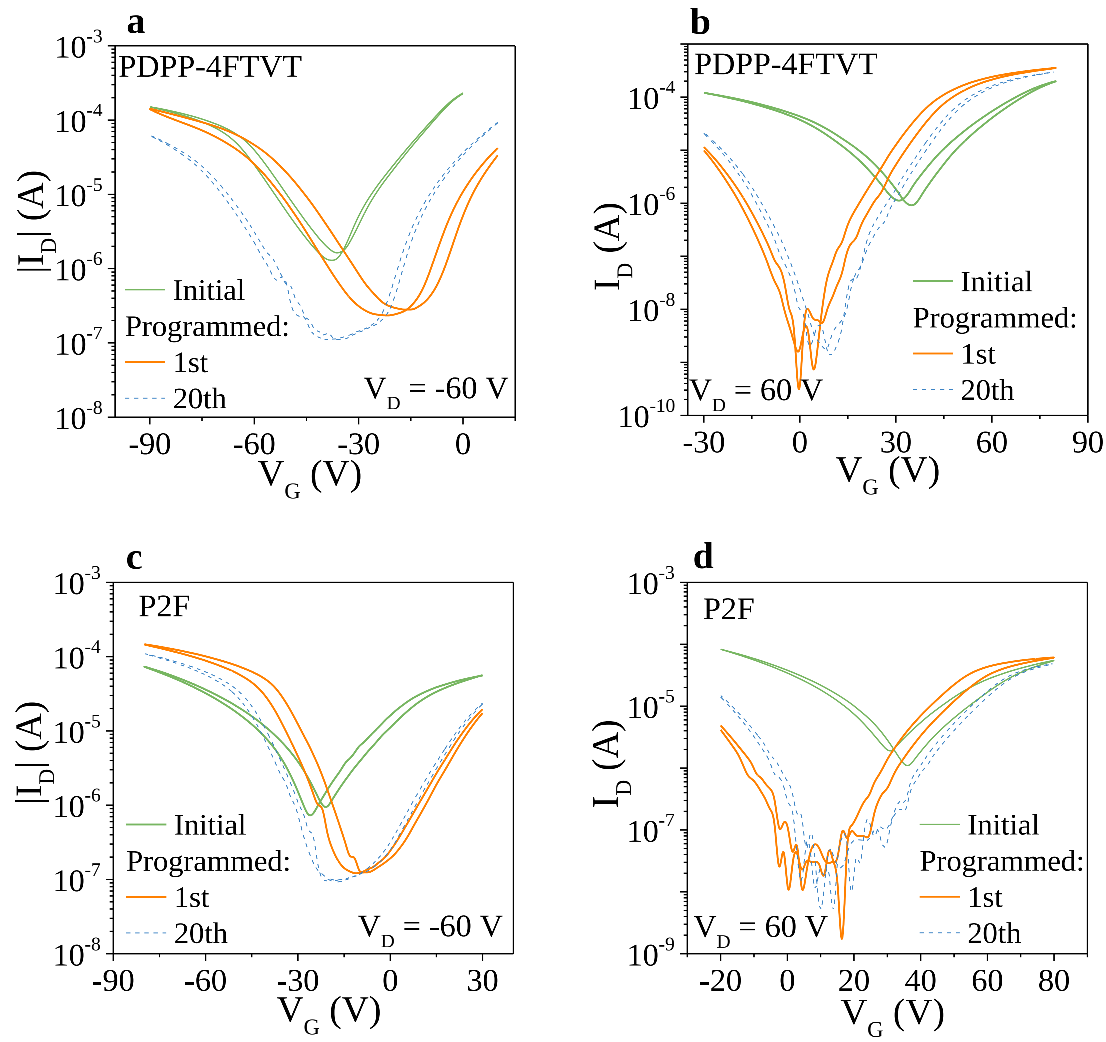

Supplementary Figure 10. Performance of ambipolar transistors based on pure **a**, **b** PDPP-4FTVT and **c**, **d** P2F films with non-uniformly distributed electret charges, which were injected by V_G = 20 V & V_D = -60 V (**a**, **c**), and V_G = -20 V & V_D = 60 V (**b**, **d**).

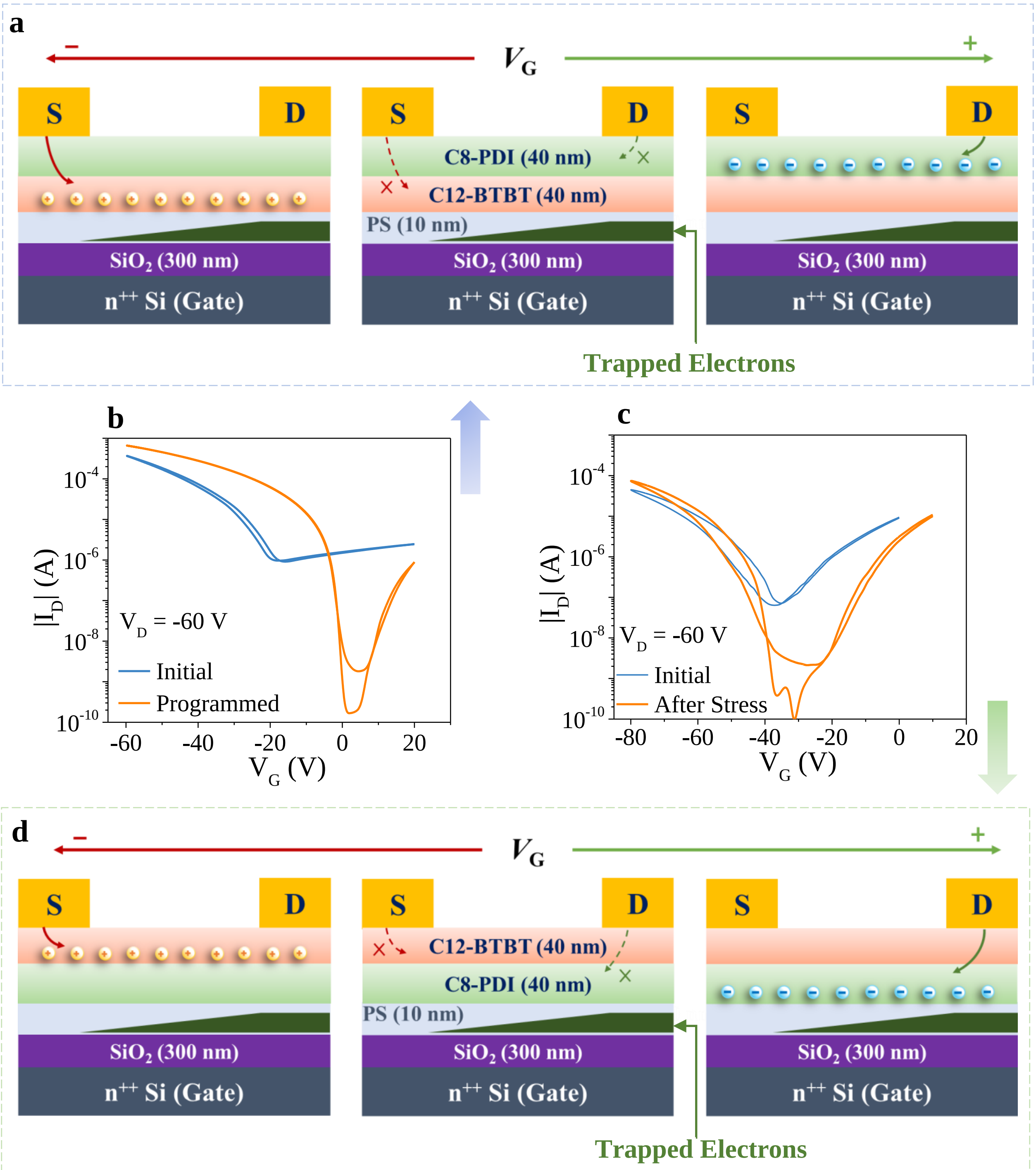

Supplementary Figure 11. Non-uniformly distributed electret charges for p-n planar heterojunction ambipolar transistors. **a** Schematic diagram of operations and **b** transfer characteristics of n-type C8-PDI top/p-type C12-BTBT bottom ambipolar transistor with non-uniformly distributed electret charges injected by V_G = 20 V & V_D = -60 V. **c** Transfer characteristics and **d** schematic diagram of operations of p-type C12-BTBT top/n-type C8-PDI bottom ambipolar transistor with non-uniformly distributed electret charges injected by V_G = 20 V & V_D = -60 V.

Supplementary Table 1. Statistics of mobility and on/off ratio of organic ambipolar transistors with nearly balanced electron and hole mobility ($1 < \mu_p/\mu_n < 5$ or $1 < \mu_n/\mu_p < 5$) under relatively high drain voltage reported in recent five years.

Material	μ_p ($cm^2 s^{-1} V^{-1}$)	μ_n ($cm^2 s^{-1} V^{-1}$)	On/Off Ratio	Reference
PTFDFT	1.08	2.23	10^2	1
2DMC	0.87	0.82	10^2	2
PDBD-Se	8.9	7.71	10^3	3
PIID-CNTVT-C1	1.14	0.59	10^3	4
RI-PDPP-CNTVT-6	1	0.87	10^3	5
PIIG-iFT2	0.12	0.05	10^2	6
PAIID-FDTE	2.94	3.27	10^3	7
PDPP3T (Split-Gate)	0.46	0.1	10^5	8
P3T4-INCN	0.15	0.05	10^5	9
PFIBI-BT	5.1	4.2	10^3	10
PBPTV	6.87	8.49	10^2	11
BTZI-BTzOR (P3)	0.34	0.5	10^1	12
P1FIID-2FBT	5.88	6.75	10^2	13
QBS/PVN	0.1	0.04	10^2	14
DPP-TT-T (Split-Gate)	0.01	0.005	10^4	15
PDPPTPT (Tri-Gate)	$1.5*10^{-4}$	$1.5*10^{-4}$	10^4	16
PBCDC	0.2	0.2	10^2	17
CNTVT:SVS (5:5)	3.15	3.03	10^1	18
DTBTff	0.44	0.15	10^3	19
IID24−CNTVT	0.26	0.83	10^2	20
P6F	2.67	2.57	10^4	21
BTBT-PA+ PTCDI-Ph	$1.06*10^{-3}$	$2.4*10^{-3}$	10^4	22
PNDI-DCS	0.42	0.447	10^5	23
PDPPF-DFT	0.26	0.12	10^3	24
PTDCNTVT-2	1.28	0.97	10^2	25
PTTDPP-DT-DTT	0.298	0.109	10^4	26
(perylene)(DBrDCNQI)	$4.2*10^{-2}$	$5.3*10^{-3}$	10^1	27
PDBPyDT2FBT	0.24	0.65	10^4	28
Y6	0.84	1.94	10^3	29
TIPS-PEN/C60	2.7	2.9	10^4	30
TiOPc	0.08	0.02	10^4	31
BPE-PTCDI/BPE-PTCDI	0.32	0.43	10^1	32
DbT-TTAR/DTTQ-11	0.83	0.37	10^1	33
PQuT-T	4.82	1.11	10^1	34
pentacene	0.2	0.26	10^1	35
PDCNBT2T	0.59	0.47	10^1	36
TPB/PCBM	0.08	0.11	10^3	37
P2DPP-TT	4.16	3.01	10^4	38
P2-A	2.4	6.3	10^1	39

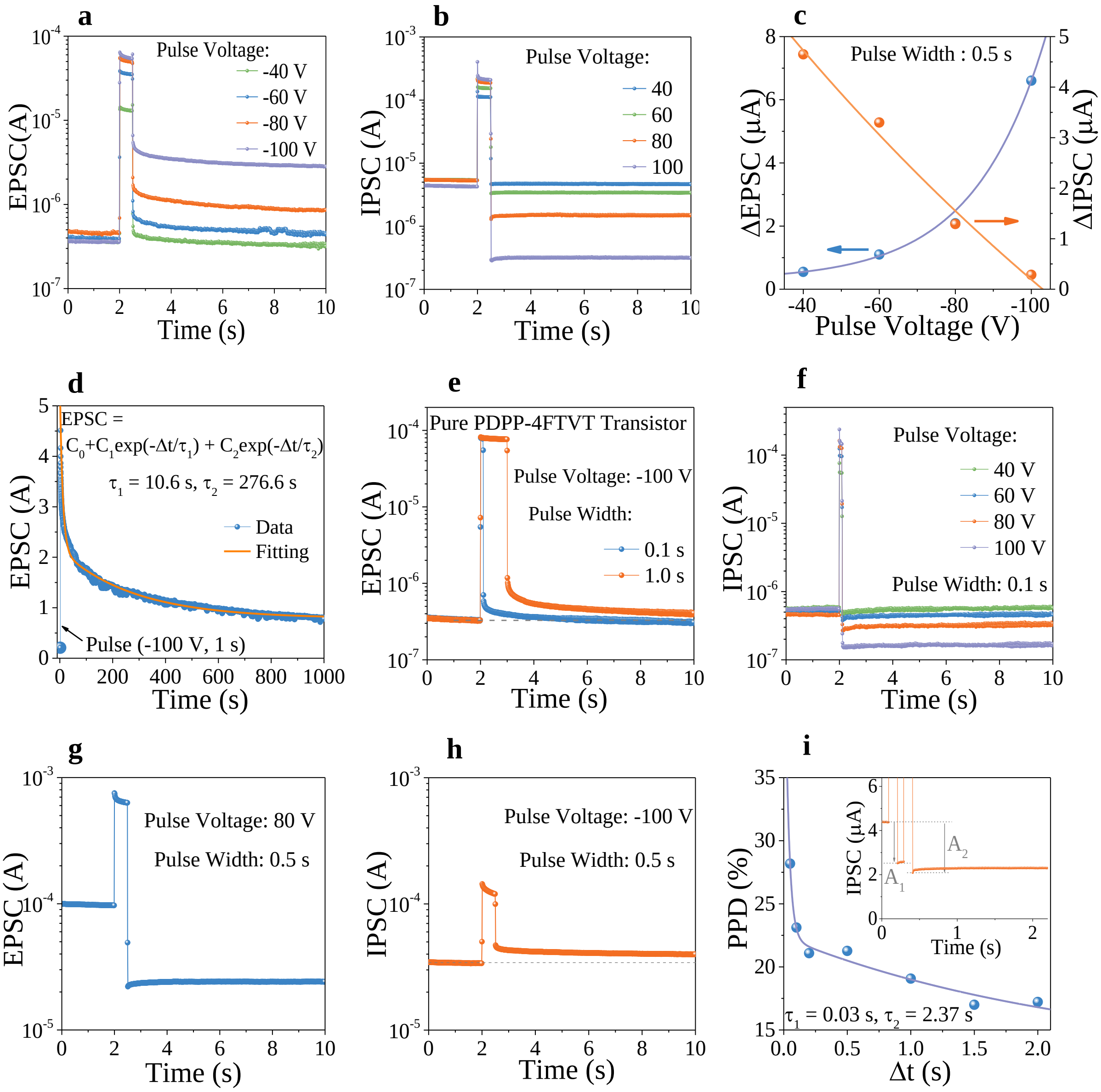

Supplementary Figure 12. **a** EPSC generated by variety of pre-synapse pulse with different pulse voltages and the same pulse width (0.5 s) for potentiation. **b** IPSC generated by variety of pre-synapse pulse with different pulse voltages and same pulse width (0.5 s) for depression. **c** Pulse voltage dependent ΔEPSC for potentiation and depression. **d** Long-term retention characteristics of EPSC generated by -100 V (1 s) pre-synapse pulse. **e** EPSC of pure PDPP-4FTVT film based synaptic transistor. **f** IPSC of PDPP-4FTVT$_{10\%}$@PS based synaptic transistor stimulated firstly. **g** IPSC and **h** EPSC of PDPP-4FTVT$_{10\%}$@PS based synaptic transistor detected at V_D = -60 V. **i** PPD (= $(A_2 - A_1)/A_1$) as a function of the pulse interval time (Δt).

References (Supplementary information)

1. Shi, D., *et al.* Half-Fused Diketopyrrolopyrrole-Based Conjugated Donor-Acceptor Polymer for Ambipolar Field-Effect Transistors. *Adv. Funct. Mater.* **30**, *1910235* (2020).
2. Zhu, X., *et al.* 2D Molecular Crystal Bilayer p-n Junctions: A General Route toward High-Performance and Well-Balanced Ambipolar Organic Field-Effect Transistors. *Small* **15**, 1902187 (2019).
3. Ni, Z., *et al.* Ambipolar Conjugated Polymers with Ultrahigh Balanced Hole and Electron Mobility for Printed Organic Complementary Logic via a Two-Step CH Activation Strategy. *Adv. Mater.* **31**, 1806010 (2019).
4. Li, D., *et al.* Tuning Charge Carrier and Spin Transport Properties via Structural Modification of Polymer Semiconductors. *ACS Appl. Mater. Interfaces* **11**, 30089-30097 (2019).
5. Li, D., *et al.* Influence of Backbone Regioregularity on High-Mobility Conjugated Polymers Based on Alkylated Dithienylacrylonitrile. *ACS Appl. Mater. Interfaces* **11**, 43416-43424 (2019).
6. Kim, M., *et al.* Controlling Ambipolar Charge Transport in Isoindigo-Based Conjugated Polymers by Altering Fluorine Substitution Position for High-Performance Organic Field-Effect Transistors. *Adv. Funct. Mater.* **29**, 1805994 (2019).
7. Chen, Z., *et al.* Multisubstituted Azaisoindigo-Based Polymers for High-Mobility Ambipolar Thin-Film Transistors and Inverters. *ACS Appl. Mater. Interfaces* **11***,* 34171 (2019).
8. Yoo, H., *et al.* Top-Split-Gate Ambipolar Organic Thin-Film Transistors. *Adv. Electron. Mater.* **4**, 1700536 (2018).

9. Kim, M.J., Lee, Y.W., Lee, Y., Woo, H.Y. & Ho Cho, J. Solvent-vapor-annealed A–D–A-type semicrystalline conjugated small molecules for flexible ambipolar field-effect transistors. *J. Mater. Chem. C* **6**, 5698-5706 (2018).

10. Jiang, Y.*, et al.* Fast Deposition of Aligning Edge-On Polymers for High-Mobility Ambipolar Transistors. *Adv. Mater.* **30**, 1805761 (2018).

11. Zhu, C.*, et al.* Regioregular Bis-Pyridal[2,1,3]thiadiazole-Based Semiconducting Polymer for High-Performance Ambipolar Transistors. *J. Am. Chem. Soc.* **139**, 17735-17738 (2017).

12. Yu, J.*, et al.* 2,1,3-Benzothiadiazole-5,6-dicarboxylicimide-Based Polymer Semiconductors for Organic Thin-Film Transistors and Polymer Solar Cells. *ACS Appl. Mater. Interfaces* **9**, 42167 (2017).

13. Yang, J.*, et al.* Isoindigo-Based Polymers with Small Effective Masses for High-Mobility Ambipolar Field-Effect Transistors. *Adv. Mater.* **29**, 1702115 (2017).

14. Kang, M.*, et al.* Ambipolar Small-Molecule:Polymer Blend Semiconductors for Solution-Processable Organic Field-Effect Transistors. *ACS Appl. Mater. Interfaces* **9**, 2686-2692 (2017).

15. Yoo, H.*, et al.* Asymmetric Split-Gate Ambipolar Transistor and Its Circuit Application to Complementary Inverter. *Adv. Mater. Technol.* **1**, 1600044 (2016).

16. Torricelli, F.*, et al.* Ambipolar Organic Tri-Gate Transistor for Low-Power Complementary Electronics. *Adv. Mater.* **28**, 284-290 (2016).

17. Park, J.-M.*, et al.* Designing Thermally Stable Conjugated Polymers with Balanced Ambipolar Field-Effect Mobilities by Incorporating Cyanovinylene Linker Unit. *Macromolecules* **49**, 2985-2992 (2016).

18. Khim, D.*, et al.* Facile Route To Control the Ambipolar Transport in Semiconducting Polymers. *Chem. Mat.* **28**, 2287-2294 (2016).

19. Barłóg, M., *et al.* Indacenodithiazole-Ladder-Type Bridged Di(thiophene)-Difluoro-Benzothiadiazole-Conjugated Copolymers as Ambipolar Organic Field-Effect Transistors. *Chem. Mat.* **31**, 9488-9496 (2019).

20. Shin, E.S., *et al.* Design of New Isoindigo-Based Copolymer for Ambipolar Organic Field-Effect Transistors. *ACS Appl. Mater. Interfaces* **10**, 13774-13782 (2018).

21. Gao, Y., *et al.* Multifluorination toward High-Mobility Ambipolar and Unipolar n-Type Donor-Acceptor Conjugated Polymers Based on Isoindigo. *Adv. Mater.* **29**, 1606217 (2017).

22. Zhao, B., *et al.* Wafer-Scale Organic Complementary Inverters Fabricated with Self-Assembled Monolayer Field-Effect Transistors. *Adv. Electron. Mater.* **7**, 2000515 (2020).

23. Ryu, H.S., Kim, M.J., Kang, M.S., Cho, J.H. & Woo, H.Y. Dicyanodistyrylbenzene-Based Copolymers for Ambipolar Organic Field-Effect Transistors with Well-Balanced Hole and Electron Mobilities. *Macromolecules* **51**, 8258-8267 (2018).

24. Sonar, P., *et al.* High-Mobility Ambipolar Organic Thin-Film Transistor Processed From a Nonchlorinated Solvent. *ACS Appl. Mater. Interfaces* **8**, 24325-24330 (2016).

25. Chen, Z., *et al.* Thiazole-Flanked Diketopyrrolopyrrole Polymeric Semiconductors for Ambipolar Field-Effect Transistors with Balanced Carrier Mobilities. *ACS Appl. Mater. Interfaces* **8**, 34725-34734 (2016).

26. Kim, M.J., *et al.* Low-Band-Gap Polymer-Based Ambipolar Transistors and Inverters Fabricated Using a Flow-Coating Method. *J. Phys. Chem. C* **120**, 13865-13872 (2016).

27. Sanada, R., *et al.* Ambipolar Transistor Properties of Charge-Transfer Complexes Containing Perylene and Dicyanoquinonediimines. *J. Phys. Chem. C* **123**, 12088-12095 (2019).

28. Li, P., *et al.* D-A(1)-D-A(2) Copolymer Based on Pyridine-Capped Diketopyrrolopyrrole with Fluorinated Benzothiadiazole for High-Performance Ambipolar Organic Thin-Film Transistors. *ACS Appl. Mater. Interfaces* **8**, 8620-8626 (2016).
29. Xiao, C., Li, C., Liu, F., Zhang, L. & Li, W. Single-crystal field-effect transistors based on a fused-ring electron acceptor with high ambipolar mobilities. *J. Mater. Chem. C* **8**, 5370-5374 (2020).
30. Zhao, X., *et al.* Organic Single-Crystalline p-n Heterojunctions for High-Performance Ambipolar Field-Effect Transistors and Broadband Photodetectors. *ACS Appl. Mater. Interfaces* **10**, 42715-42722 (2018).
31. Zhang, Y., Wei, X., Zhang, H., Chen, X. & Wang, J. Ambipolar organic transistors with high on/off ratio by introducing a modified layer of gate insulator. *Appl. Surf. Sci.* **427**, 452-457 (2018).
32. Zhang, X., *et al.* Precise Patterning of Laterally Stacked Organic Microbelt Heterojunction Arrays by Surface-Energy-Controlled Stepwise Crystallization for Ambipolar Organic Field-Effect Transistors. *Adv. Mater.* **30**, 1800187 (2018).
33. Vegiraju, S., *et al.* Solution-Processed High-Performance Tetrathienothiophene-Based Small Molecular Blends for Ambipolar Charge Transport. *Adv. Funct. Mater.* **28**, 1801025 (2018).
34. Kim, Y., *et al.* pi-Conjugated Polymers Incorporating a Novel Planar Quinoid Building Block with Extended Delocalization and High Charge Carrier Mobility. *Adv. Mater.* **30**, 1706557 (2018).
35. Park, B., *et al.* Anomalous Ambipolar Transport of Organic Semiconducting Crystals via Control of Molecular Packing Structures. *ACS Appl. Mater. Interfaces* **9**, 27839–27846 (2017).
36. Shi, S., *et al.* Cyano-substituted benzochalcogenadiazole-based polymer semiconductors for balanced ambipolar organic thin-film transistors. *Polym. Chem.* **9**, 3873-3884 (2018).

37. Zhao, X., *et al.* Organic Single-Crystalline Donor-Acceptor Heterojunctions with Ambipolar Band-Like Charge Transport for Photovoltaics. *Advanced Materials Interfaces* **5**, 1800336 (2018).
38. Yang, J., *et al.* Bis-Diketopyrrolopyrrole Moiety as a Promising Building Block to Enable Balanced Ambipolar Polymers for Flexible Transistors. *Adv. Mater.* **29**, 1702115 (2017).
39. Di Pietro, R., *et al.* Synthesis of High-Crystallinity DPP Polymers with Balanced Electron and Hole Mobility. *Chem. Mat.* **29**, 10220-10232 (2017).